# An Error Analysis Model for Adaptive Deformation Simulation

Umut Koçak, Karljohan Lundin Palmerius, and Matthew Cooper
*C-Research*
*Linköping University, ITN*
*Norrköping, SWEDEN*
*Email: umut.kocak@liu.se, karljohan.lundin.palmerius@liu.se, matthew.cooper@liu.se*

***Abstract*—With the widespread use of deformation simulations in medical applications, the realism of the force feedback has become an important issue. In order to reach real-time performance with sufficient realism the approach of adaptivity, solution of different parts of the system with different resolutions and refresh rates, has been commonly deployed. The change in accuracy resulting from the use of adaptivity, however, has been been paid scant attention in the deformation simulation field. Presentation of error metrics is rare, while more focus is given to the real-time stability. We propose an abstract pipeline to perform error analysis for different types of deformation techniques which can consider different simulation parameters. A case study is also performed using the pipeline, and the various uses of the error estimation are discussed.**

***Keywords*-physically based; deformation; multi-resolution; perception; error; analysis.**

## I. Introduction

The integration of haptics, the sense of touch, in human computer interaction has increased the immersion effect of virtual environments. Haptics has been used to serve different aims such as guidance, visualization, and realism in various computer applications. Considering the growing use of haptics in medical applications, such as in virtual simulations for training and rehearsal purposes, the degree of realism has become a crucial issue.

Achieving a compromise between realism and stability has always been a major challenge in haptics, especially for deformable objects. High refresh rates (1 kHz) are necessary to achieve a stable and continuous force feedback, while solution of the physical models with desired resolutions comes with a heavy computational burden. Adaptive multiresolution techniques have been among the most popular methods proposed to achieve desired refresh rates with required resolution. A major problem with this approach, however, has been a lack of focus on the reduced realism due to the error introduced by adaptivity, and the lack of standard error metrics.

In the literature it can be seen that consideration of the error is usually superseded by stability concerns but there are some error estimation techniques, widely studied in the context of Finite Element Methods (FEM) (e.g., [1], [2], [3], [4]), and adaptive studies [5] suitable for real-time use. Exploiting such methods to choose optimal solutions which minimize error while maintaining sufficient performance to ensure stability would be beneficial. The common approach in the real-time deformation simulation field, however, is simply to include the maximum number of nodes which can be solved in real-time while keeping the simulation stable. Presentation of numerical values for the element sizes, time-steps and how they affect the accuracy is rare, however. One possible reason is the fact that estimating an error is not a trivial process, especially for adaptive simulations which vary parameters in real-time. In addition to deciding which parameter to consider (strain, stress, force) for error estimation, one also has to choose a reference. Therefore presentation of the numerical values without any error analysis is usually avoided in the literature.

In this study, we propose a pipeline used to analyze force feedback error caused by adaptive solution of deformation simulation. The idea depends on creating an offline error mapping of a deformation model for a set of parameters such as user inputs, material properties and adaptivity parameters. The potential uses of the offline error mapping include: (1) surveying correlations between error and parameters, (2) real-time quality assessment, and (3) real-time parameter adjustment to keep the error below some desired limits. The pipeline is applied in a case study by performing experiments in the simulation environment.

The outline of the paper is as follows: related work and theoretical background are presented in the second and third sections, respectively. The motivation for the work is discussed in the fourth section, followed by the explanation and the case study of the pipeline in the fifth and the sixth sections. The conclusions are presented in the final section of the paper.

## II. Related Work

The main challenge in deformation simulation is reaching sufficient realism while maintaining the desired refresh rates. There are a variety of different deformation models and optimization techniques available. Among the deformation models, FEM is commonly considered to provide the most realistic behaviour and so, despite the substantial computational load it incurs, is the focus of most optimization and error analysis studies. In this section studies about adaptivity applied to FEM and the error analysis are summarized.

 ISBN: 978-1-61208-177-9 

A common technique to achieve sufficient performance while retaining required realism around the point of contact is adaptivity. There are several approaches (for example [5], [6], [7]) which exploit adaptive spatial multiresolution models to keep the accuracy higher around the contact point while reducing computational load in the less precisely modelled parts.

Despite this frequent use of adaptive element size and time-step, the effects of such approaches on the perceived force feedback have not been comprehensively surveyed. The common method in real-time applications is, if error is considered at all, to use an error measure for each element and adapt the element size and the time-step for elements. The error estimation has, however, been more thoroughly studied in FEM (i.e, [1], [2], [3], [4]) although the real-time aspect is not, generally, as important there. Designing an 'ideal-error-estimator-solution' which is reliable and sufficiently computationally inexpensive that it can be used in real-time is an unsolved issue, as discussed in [3].

In this study, we propose a general pipeline to analyze the behaviour of the force error with respect to the level of detail in both time and spatial domains. The direct relationship between the force response and the solution of the whole model with different frequencies was presented in [8] for mass-spring models. In the pipeline we propose, the error can be analyzed for different deformation models and different parameters, such as material properties, and input types. An analysis of the error for a special case is also presented.

## III. Background: Stability and Accuracy

The deformation simulation on a mesh depends on discretizing a continuous domain into elements. In addition, the iterative solution of the resulting differential equations depends on discrete time-steps. There are two main issues to be considered in the discretization: stability and accuracy. The adjustment of element size and and time-step includes a compromise between these two concepts, therefore adaptive simulations should take these two concepts into consideration in real-time. Keeping the simulation stable means having a deformation model which always converges to the result. The accuracy, on the other hand, affects the error in the deformation.

### A. Stability

The deployment of iterative solvers is generally preferred over analytical ones in deformation simulation because of their superior speed. The iteration process requires the choice of a time-step, which affects the accuracy and stability of the simulation. The two main categories of iterative solvers, implicit and explicit, have different behaviour in terms of stability. Implicit solvers are unconditionally stable, which means that the solution converges to the final value no matter how large the time-step. On the other hand, the time-step is limited in the case of explicit solvers, where having an eigenvalue of greater than 1 in the stiffness matrix will result in divergence. The time-step limit depends on the maximum natural frequency which, in turn, depends on the material properties and the element size. The time-step limit can be physically interpreted to be that it must be small enough that no information propagates more than one mesh element per step. To achieve stability it is therefore necessary to consider the time-step and the element size together.

### B. Accuracy

Increasing the time-step results in increasing error. In the case where a single ordinary differential equation is considered, the time-step is crucially important to achieve acceptable accuracy. In the case of a large number of differential equations, however, keeping the time-step just under the stability limit provides sufficient accuracy. The reason for this is the fact that a stiff system of differential equations covers a wide spectrum of natural frequencies. The stability limit is evaluated with respect to the highest frequency of the system. Therefore for a time-step which is close to the critical stability time-step limit, the response of the model for the highest frequencies will not have high accuracy. Fortunately, the structural response of the objects is dominated by much lower frequencies which are sufficiently more accurate for the chosen time-step. Therefore, for explicit solutions of a large number of equations, the accuracy is not an issue as long as the stability condition is satisfied [9].

The discretization in the spatial domain is another factor affecting accuracy. For instance, in case of FEM, the type, shape and size of the elements also play a role in the accuracy. Once the shape of the element is chosen, the order of the polynomial used to calculate the shape functions of the element can also vary. While increasing the order results in higher accuracy, using lower orders is common in real-time applications because of its drastic effect on the stability condition. The error of a quantity is of the order of $\mathcal{O}(h^{p+1-m})$ [10]; where $h$ is the element size, $p$ is the degree of the polynomial used to calculate shape functions, and $m$ is the order of the highest derivative in the governing equilibrium equation expressed in terms of displacements.

## IV. Motivation

The common approach followed in deformation simulations is to choose the maximum time-step which guarantees stability for a given mesh resolution. As long as the stability conditions are satisfied, the accuracy criteria are also satisfied for large deformable meshes, as discussed in the previous section. It is not only the time-step but also the element size which affects the accuracy of the deformation behaviour. In real-time deformation simulation studies, it is usually considered to be sufficient to include the number of nodes required for the mesh to be solved stably. The presentation of numerical values for the element sizes and how they affect the accuracy, however, is rare in this field.

Another issue which has been largely ignored in adaptive haptic applications where both the resolution and time-step are adjusted in real-time, is the potential to exploit the perception limits of human beings for optimization purposes. There have been numerous studies which have surveyed the different human perception limits but ways to exploit these limitations in hardware and software solutions are rarely explored. The research (for example [11], [12]) shows that there are just-noticeable-differences in force magnitude and in force direction. The threshold for force magnitude has been found to be around 7% in [11]. Similarly, the average force direction discrimination thresholds are 18, 26, and 32 degrees, depending on the accompanying visual input [12]. One could exploit these thresholds to save computational power by simplifying the force calculation while ensuring that the error in the force remains below the limit of perceivability.

In this work we propose a pipeline which analyzes the error due to the various parameters, including adaptivity parameters, and deploys a mechanism, without additional computational burden, to control the simulation parameters in real-time, according to the error criteria.

## V. Perceptual Adjustment Model

In order to introduce the facility to adjust the computational complexity without perturbing the user's perception of the represented forces it is necessary to examine the explicit correlation between force error and parameters, assessing quality of simulation at run-time, and adjusting adaptivity parameters to maintain the error under desired limits. The abstract pipeline is explained in this section while a case study performed by experiments is presented in the next section.

### A. Error Identification Principle

Achieving exact solution in real life scenarios is very rare for deformation simulations. There are several steps in the process contributing to the error, such as modelling, discretization and numerical errors. The pipeline proposed in this study focuses on the error caused by the deployment of adaptivity with varying element sizes and time steps in the simulation. In addition, a so-called goal-oriented [3] approach is followed by analysing the force feedback error of a contact node. In other words, the error considered in this model refers to the force error introduced by varying element sizes and time-steps while one must keep in mind the other contributions to the total error. For a given mesh and deformation model, the solution for the whole mesh with the highest resolution, and with a sufficiently low enough time-step to maintain stability, is considered as a 'reference' force with no error.

### B. Offline Error Characterization

The idea of calculating an offline error mapping depends upon applying Monte Carlo simulation for a set of parameters to obtain a force feedback value for each sample. One needs to maintain stability while varying the tested parameters in a reasonably wide range. To maintain stability, the time-step needs to be smaller than a critical time-step which depends on a number of parameters including the element size, elasticity, mass and poisson ratio. This causes different stability behaviour in the simulation for different materials. The choice of time-step for real-time solutions is also dependent on the computational power available and the number of nodes required. Considering the limitations on the time-step and its effects on the range of parameters to be tested, offline deformation solutions are preferred to create the error mapping. This allows the exploration of time-steps decoupled from the limits imposed on computational power and number of nodes in addition to maintaining the stability for a wide range of parameters for a given time-step.

The idea of offline error mapping is illustrated in Figure 1. The pipeline uses a number of types of input parameters to a chosen deformation model and creates an error mapping specific to these parameters which can be categorized as user input, material properties and adaptive simulation parameters. The amount of strain, input frequency, and choice of contact node can be named as examples of user input. The material properties include the physical properties of the object such as elasticity, mass, poisson ratio, or damping, while the deformation model can be any deformation algorithm such as FEM, mass-spring etc. The adaptive simulation parameters include the distribution of element sizes and time steps throughout the mesh.

The first step in creating the error mapping is an offline evaluation of the reference force explained in Section V-A for a range of user input and material properties parameters. The force feedback is then calculated again for the same set of parameters but deploying adaptivity with varying element sizes and time-steps. The force feedback obtained by deploying adaptivity for this set of parameters is compared with the corresponding reference force, evaluated without adaptivity, to calculate the error. This procedure applied to a specific case is explained in more detail in Section VI-C.

### C. The Uses of Error Mapping

One of the potential uses of an error mapping is surveying explicit correlation between force error caused by adaptivity and material or input parameters. This might be used to gain more insight about the effects of adaptivity for different deformation models and materials leading to better choices of algorithms for different types of applications. Another use would be assessing quality of simulation at run-time without a major computational burden. Since the error mapping has been pre-calculated offline, the only extra work introduced is to find the corresponding error in real-time, by using a

 ISBN: 978-1-61208-177-9 

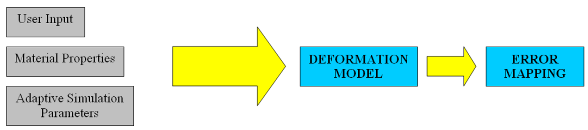


Figure 1. The offline error mapping procedure: The user input, material properties and adaptive simulation parameters are given as input to the deformation model. The force feedback for each trial is compared with the solution of the whole object with highest resolution and an error mapping is created for each trial.

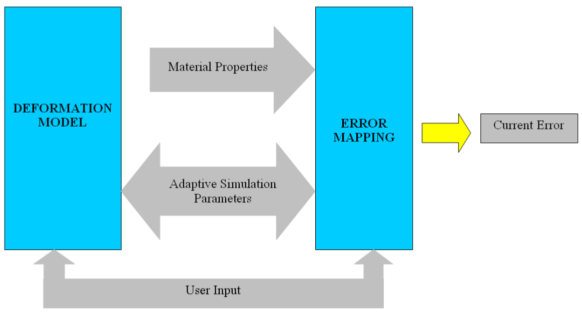


Figure 2. The online error assessment and quality adjustment: For a given set of material properties, adaptive simulation parameters and user input, the error mapping is used to determine the current error. This can either be used purely for quality assessment purposes or the adaptive simulation parameters can be fed back to the deformation model at run-time aiming for a compromise between target error value and stability.

lookup table, as described in the results section. Figure 2 illustrates the online uses of the error mapping. In addition to just evaluating the current error for assessment purposes, the adaptive simulation parameters can be adjusted and fed back to the deformation model in order to to maintain the error under desired limits. This real-time adjustment, however, has to consider the stability issues which are coupled with the available computational power to achieve a compromise between error and stability. In the event that both constraints cannot be simultaneously met during real-time use, the system must ensure that stability is retained while recording the fact that the error limitations have been exceeded and, perhaps, informing the user that this failure has occurred.

## VI. Experiments

Experiments have been performed to apply the abstract pipeline proposed to a specific scenario for a chosen deformation model and a set of parameters. We foresee no obstacles to applying the same principles and performing a more elaborate analysis by extending the number of parameters.

Linear FEM, where performance is a less serious concern compared with non-linear FEM, was chosen as the deformation model. The adaptive solutions, however, are still needed for larger numbers of nodes even for linear FEM. Considering the deformation characteristics in real life situations, complex properties such as viscoelasticity

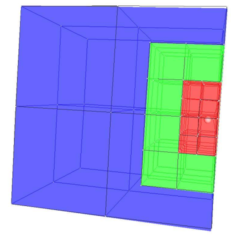

Figure 3. The allocation of asynchronous regions in the object. Different regions have different mesh resolutions in addition to being solved with different time-steps. The primary region (local neighbourhood of the contact) is shown with red, and the secondary regions are shown in green and blue.

and anisotropy are also commonly observed in addition to non-linearity. The error analysis for tissue deformation is, therefore, a non-trivial process which needs to consider different physical properties. The reason we chose the linear FEM is to make the proof of concept of the pipeline in a relatively simpler model, and analyze more complex models as future work. Clearly the structure of the pipeline presents no obstacles to either changing the deformation model or extending the set of parameters.

### A. Deformation Model

A dynamic linear finite element model with a cubic element is used. The simulation time is discretized into time-steps to evaluate the numerical integration of (1):

$$\mathbf{M}\ddot{u} + \mathbf{C}\dot{u} + \mathbf{K}u = f \tag{1}$$

where the stiffness, mass and damping matrices are represented by **K**, **M**, and **C** respectively, while $u$, $\dot{u}$, $\ddot{u}$ and $f$ refer to displacement, velocity, acceleration and force vectors. The mass matrix is diagonalized and a constant damping for each node is used. The reader is encouraged to see [10] for further details of the finite element method.

### B. Parameters

**Adaptive Simulation Parameters:** There are different ways to implement adaptive deformation (for example [5], [13]). In our framework the deformation is calculated with different resolutions and at different update rates for different regions of the object. The local neighbourhood of the contact point maintains higher resolution and smaller time-steps than the more remote regions, illustrated in Figure 3. The corresponding FEM equations for different regions are solved asynchronously with different time-steps and resolutions. The regions, therefore, are referred to as *asynchronous regions*. Throughout the rest of the paper the local neighbourhood of the contact node, having the highest frequency, will be referred as *the primary region* and the others as *the secondary regions*. The framework used allows real-time adaptation of regions and their sizes

 ISBN: 978-1-61208-177-9 

as the nature of the contact is changed. The details of the implementation, however, are out of the scope of this study and the reader can see different examples of adaptive simulations (for example [5], [13]) for further details.

In this system, the force at the contact node depends on the resolutions, time steps and the sizes of the regions. Two asynchronous regions have been employed throughout the experiments presented here. The primary region's spatial and time resolution has been fixed for all experiment sets. The spatial resolution (2.5 cm) has been chosen to be the highest resolution used during the reference force calculation without adaptivity and the time-step has been kept at 1 kHz throughout for the primary region.

The secondary region frequency is one of the parameters being varied using rates of 1 kHz, 900, 800, 700, and 600 Hz. The use of lower time-steps was possible for some of the data sets, however not for all. For a given resolution, for instance, the refresh rates need to be higher for more stiff materials, or lower mass densities. In order to be able to analyze a wider range of parameters, higher stiffness or lower mass densities, with the same frequency values the refresh rates were chosen to be high. As explained in Section III-B, the accuracy is not affected by the time-step as long as the stability criteria are met. This is also observed in the results showing that the frequency does not affect the error. The choice of high refresh rates to cover a wider range of material properties therefore has no effect on the error analysis.

The resolution of the the secondary region is another parameter under consideration and has been varied over multiples of the primary region resolution which are $1\times$, $2\times$, and $3 \times 2.5$ cm.

The third parameter surveyed is the size of the primary region. The size has been measured as the number of nodes in all directions from the contact node homogeneously and changed between 1, 2, 3 and 4 in three dimensions. To illustrate, a region with value of 1 as size includes $3 \times 3 \times 3$ nodes in three dimensions, including the contact node.

**User Input:**

To apply a deformation to the model, a simulated haptic device was used allowing the application of a precise and reproducible input. While it is possible to apply deformation to a chosen set of contact nodes, the deformation was applied to a fixed contact node throughout the experiments. Two parameters have been changed for the deformation applied: Strain and frequency. To obtain a realistic response from linear FEM the maximum amount of strain applied has been kept limited, typically to less than 10% [14] of the mesh size. The amount of strain has been chosen to be 0.5, 1.0 or 1.5 cm. The frequency of the input has been changed between 0.5, 1.0 and 1.25 Hz.

**Material Properties:** Physical properties like elasticity, mass, damping and poisson ratio have been varied during the experiments. The ranges have been chosen according to the soft tissue properties described in the literature. The elasticity values measured in the different studies are: between 5 and 35 kPa in [15], 6 and 11 kPa in [16], 0 and 3.5 kPa in [17]. The differences between the results of the studies mentioned are due to the tissue type, the magnitude of deformation, the non-linear behaviour of the elasticity and the level of precompression as discussed in [18]. Consequently, the elasticity has been set to 5, 10, 15 and 20 kPa in the experiments. The mass density has been found to be 1 g/cm$^3$ in [19] and was set to 0.8, 1.0 and 1.2 g/cm$^3$ for the experiments. Measurement and modelling of the damping for soft tissue is non-trivial since the coefficient depends on stress level [9] and vibration frequency. The damping for a human thigh has been measured for different applied force magnitudes and frequencies and angles of flexion of the knee in [20]. The damping varies between 7 and 102 s$^{-1}$ for a force applied normal to the skin. The response of the deformation behaviour in pilot studies was also considered while deciding the damping values and they were set to 10, 20, 30 and 40 s$^{-1}$ during the experiments. Poisson ratios of both fat and muscle tissue have been measured to be approximately 0.49 in [21] and have been set to 0.40, 0.45 and 0.49 for the experiments.

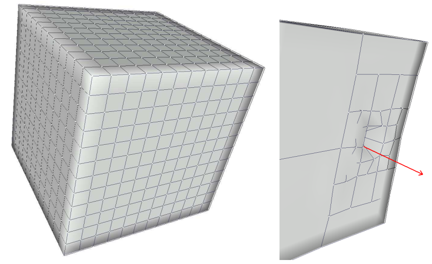

Figure 4. The experiments have been performed with a cube composed of $13 \times 13 \times 13$ nodes. The deformation is shown on the right half side of the figure.

*C. Procedure*

A deformation is applied to the model by a simulated haptic device which provides a precise and reproducible input. A reference force is evaluated at the contact node by solving the whole mesh without any adaptivity. The same input is then applied by employing two asynchronous regions with varying parameters. The force responses of the asynchronous regions are compared to the reference force to obtain an error value. This procedure is repeated for the full set of ranges of material user input and material parameters.

A cube, shown in Figure 4, with edge length of 25 cm and $13 \times 13 \times 13$ nodes is used for the experiments. The four corner nodes on the back face are fixed and input is applied to the middle node on the front face. For deformation, an explicit central-difference solver is employed with cubic finite element type together with linear FEM.

 ISBN: 978-1-61208-177-9 

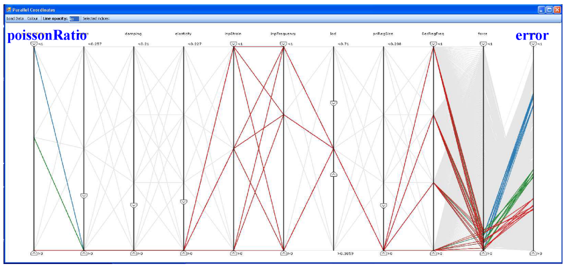


Figure 5. Parallel coordinates allow restriction of some parameters in order to observe the effects of the others. The use of colours enables the observation of how each parameter affects the error. In this case the material properties other than poisson ratio, resolution of secondary region and primary region size are fixed, and colours are used to distinguish the effect of poisson ratio on the error. The right-most axis is error and the left-most the poisson ratio. The colours identify three different levels of poisson ratio.

Table I
THE PARTIAL CORRELATION BETWEEN ERROR AND THE PARAMETERS

| | Error Correlation | | | |
|---|---|---|---|---|
| | Pearson | | Spearman | |
| | Coefficient | p | Coefficient | p |
| Poisson Ratio | 0.5837 | 0 | 0.5488 | 0 |
| Mass | 0.0166 | 0.0001 | 0.0053 | 0.2152 |
| Damping | 0.0216 | 0 | -0.1691 | 0 |
| Elasticity | 0.4746 | 0 | 0.2712 | 0 |
| Input Strain | 0.4377 | 0 | 0.158 | 0 |
| Input Frequency | 0.0119 | 0.0058 | -0.1244 | 0 |
| Level of Detail | 0.4582 | 0 | 0.7033 | 0 |
| Pr. Reg. Size | -0.5624 | 0 | -0.6243 | 0 |
| Sec. Reg. Freq. | -0.0015 | 0.7354 | 0.0003 | 0.9403 |
| Force | -0.5073 | 0 | -0.1827 | 0 |

### D. Results

The error mapping obtained can be used to analyze the effect of each parameter on the force, seperately. The correlations between the error and the individual parameters are presented in this subsection. A data set consisting of 62208 sample points has been obtained by a Monte Carlo simulation. After elimination of the divergent sets, the number was reduced to 54083 samples. Visualization techniques and statistical tests have been used to analyze the data.

Parallel coordinates, as illustrated in Fig. 5, are used to visualize the effect of each variable on the force. The use of parallel coordinates allows the user to keep all of the parameters but one fixed or restricted so that the effects of the free parameter on the error can be observed. Parallel coordinates provide a general picture of how the error is affected by each parameter. However, to convey a quantified measurement between the error and the parameters, statistical tests can be performed. Two different partial correlation tests have been carried out.

To observe how the error is affected by a single parameter, eliminating the effects of the other parameters, two common partial correlation tests are applied. Table I illustrates the correlation coefficients of error and the p-values for each parameter obtained by the Pearson and Spearman tests. The former is suitable for linear relations and assumes normal gaussian distribution for each variable. Since the ranges used during the experiments do not meet the gaussian distribution requirement, and the linearity of the relations cannot be known in advance, the Spearman test is more suitable for the data. If the Spearman parameter is larger than the Pearson in absolute value, however, one can conclude that the variables are consistently correlated but not in a linear fashion. The correlation coefficient varies between -1 and 1. The higher the absolute value of the coefficient the more correlated the parameters are with the error. To determine the significance of covariance, a t-test with a confidence level of 95% is typically applied, the p-values of which are also presented in Table I. P-values below 0.05 can be interpreted as indicating that the correlation is very unlikely to be different from zero by chance. The correlation coefficients are interpreted as small between 0.0 and 0.1, medium between 0.1 and 0.3, and large between 0.5 and 1.0 [22].

For the scenario considered in these experiments, the analysis of the correlation indicates the following. Amongst the material properties, the poisson ratio is the one most correlated with the error with a p-value of $< 0.01$. Increasing the poisson ratio causes the error to increase significantly. One cannot say the same for the mass from the p-value. Therefore parallel coordinates are used to manually check the relationship between the mass and the error, and it can be said that no visually observable significant change occurs in error due to changing mass. The elasticity has a positive, and the damping has a negative correlation with the error, but neither is as strong as that of the poisson ratio.

Of the input parameters, frequency and strain show negative and positive correlation, respectively. The strength of the correlations are not, however, significant and they can be grouped into medium correlation.

One can see the high positive and negative correlation with the element size of the secondary region and the primary region size, respectively. Both correlations can be said to be nonlinear since the Spearman coefficient is larger than the Pearson. The refresh rate of the secondary region has no correlation with the error. This can be explained by the fact that, as explained in Section III-B, a small enough time-step for stability also satisfies the accuracy criteria as long as the solution system is stiff enough [9].

### E. The Real-Time Uses of Error Mapping

The error mapping can be used to determine the force error in real-time. This can allow some simulation parameters to be adjusted to keep the error below limits such as those set by human perception. The adaptive simulation parameters, such as element size and time-steps, can be

 ISBN: 978-1-61208-177-9 

adjusted depending on the error. The material properties are measured physical values and the input parameters are determined by the user. These two should be used in obtaining the real-time error from the mapping rather than being adjusted to achieve a desired error.

Real-time determination of the error from the error mapping might be non-trivial and depends on how the mapping is obtained. A look-up table, as shown in Table II, is then used to determine the error for the current parameters and simulation state. Some issues such as continuously varying input frequency, heterogeneous material properties or changing contact node might require special solutions during the error mapping lookup phase.

The real-time measurement of input frequency may not be practical, instead one can exploit the fact that human beings have limited bandwidth while touching objects. An upper bound for a force control was found to be 25 Hz in [23] and 20 Hz in [24]. From the human output perspective 10 Hz is considered to be more than sufficient according to [25]. For the presented error mapping in the example, the lowest input frequency results in the highest error. Therefore the lowest frequency can be considered to determine a maximum bound for the effect of input frequency on the error.

Another issue is the deformation of objects with heterogeneous material properties making the use of a look-up table non-trivial. One alternative to address this problem is to check the material properties within a local neighbourhood and consider the combination of material properties with the highest error in the neighbourhood. For example considering the maximum elasticity, poisson ratio and minimum damping will ensure the error constraint is on the safe side by assuming the worst case scenario. Another alternative, which is less safe, would be to take average of each material property within the local neighbourhood to determine error. The limitation of this technique is the existence of rigid sub-objects, the effects of which on asynchronous regions will be explored in future studies.

The number of contacts considered during the creation of the error mapping determines how elaborate the mapping is. Creating an error mapping for each node in the mesh can be quite expensive. A mapping with few nodes and real-time interpolation of the error between these nodes provides an error value for each node of the mesh.

## VII. Conclusions and Future Work

In this study, we have proposed a pipeline to survey the varying accuracy of the force feedback due to adaptivity with respect to a number of parameters of a deformation model. First, an error mapping with respect to certain number of parameters, including user inputs, material properties and adaptive simulation parameters is created. The deformation is first solved off-line for the whole object with the highest resolution mesh and the force response saved as a reference. The adaptivity is then employed with different parameters and the force output is compared with the reference force to estimate an error for the given parameters. This procedure is repeated for a range of different material properties, and user inputs. In addition to providing an error measure without any serious real-time computational burden, the offline solution of the deformation decouples computational power from the stability requirement. The whole stable range of parameters for a given deformation model can, therefore, be solved offline and conveyed through the error mapping.

Table II
The look-up table for the error

| Material Prop. | | | | Applied Input | | Asynch. Reg. | | |
|---|---|---|---|---|---|---|---|---|
| P.R. | M | D | E | Strain | Freq. | Lod | Pr.Reg | Err |
| 0.49 | 0.8 | 10 | 5000 | 0.005 | 0.5 | 2 | 1 | 56.7 |
| 0.49 | 0.8 | 10 | 5000 | 0.005 | 0.5 | 2 | 2 | 15.7 |
| 0.49 | 0.8 | 10 | 5000 | 0.005 | 0.5 | 2 | 3 | 8 |
| 0.49 | 0.8 | 10 | 5000 | 0.005 | 0.5 | 2 | 4 | 1.6 |
| 0.49 | 0.8 | 10 | 5000 | 0.005 | 0.5 | 3 | 1 | 66.7 |
| 0.49 | 0.8 | 10 | 5000 | 0.005 | 0.5 | 3 | 2 | 60.4 |
| 0.49 | 0.8 | 10 | 5000 | 0.005 | 0.5 | 3 | 3 | 6.8 |
| 0.49 | 0.8 | 10 | 5000 | 0.005 | 0.5 | 3 | 4 | 4.1 |
| 0.49 | 0.8 | 10 | 5000 | 0.005 | 1.0 | 2 | 1 | 60 |

The error mapping obtained offline can be used to survey the correlation between force error and material properties, user input and adaptive simulation parameters. One can compare how different deformation models, such as linear FEM, non-linear FEM, or mass-spring are affected by adaptivity. This exploration has the potential to help in choosing algorithms and adaptivity parameters for different types of application. At run-time the quality of the force feedback can be continuously monitored with the help of error mapping, allowing the adaptive parameters to be adjusted to keep the error below the desired limits while maintaining stability.

Experiments have been performed on an example application of the proposed pipeline. The error mapping was created for a linear FEM. Material properties such as elasticity, mass density, damping, poisson ratio and user input parameters like strain, input frequency have been changed in addition to adaptive simulation properties. Observed correlations between the error and the input parameters have been presented and an example use of a look-up table for error mapping in real-time was proposed.

One must keep in mind that the example presented in the experiments section is a special case of the pipeline proposed in this study. In real life situations, more complex material properties such as nonlinearity, viscoelasticity, or anisotropy are commonly observed. Consequently achieving an ideal error estimation is non-trivial [3] in deformation simulation. We used a linear FEM to visualize an application of the pipeline because of its relatively simple structure. The possible challenges that might occur during the real-time use of the error mappings for models exhibiting material inhomogeneity, interpolation of error for contact nodes, and corresponding solutions have also been discussed.

In future work we will study the pipeline with alternative parameters and deformation models. The effect of different contact nodes, shapes, the use of mapping for heterogeneous materials, nonlinearity, and viscoelasticity can be named among the concepts to be surveyed. A user-centred study employing the error mapping with just noticeable differences will be very interesting to study in the subsequent phases.

## Acknowledgments

We thank Camilla Forsell for her help with the statistical analysis applied in this work. This work has been funded by the Swedish Science Council through grant number 621-2005-3609, the Foundation for Strategic Research (SSF) under the Strategic Research Center MOVIII, and the Swedish Research Council Linnaeus Center CADICS.

## References

[1] M. Bercovier and O. Pironneau, “Error estimates for finite element method solution of the stokes problem in the primitive variables,” *Numerische Mathematik*, vol. 33, pp. 211–224, 1979.

[2] E. Rank and O.C. Zienkiewicz, “A simple error estimator in the finite element method,” *Communications in Applied Numerical Methods*, vol. 3, pp. 243–249, 1987.

[3] T. Gratsch and K.J. Bathe, “A posteriori error estimation techniques in practical finite element analysis,” *Computers & Structures*, vol. 83, pp. 235–265, 2005.

[4] M.J. Aftosmis and M.J. Berger, “Multilevel error estimation and adaptive h-refinement for cartesian meshes with embedded boundaries,” in *40th AIAA Aerospace Sciences Meeting and Exhibit, AIAA Paper*, 2002.

[5] G. Debunne, M. Desbrun, M. Cani, and A. Barr, “Dynamic real-time deformations using space & time adaptive sampling,” in *Proc. Annual conference on Computer Graphics and Interactive Techniques (SIGGRAPH 01)*, 2001, pp. 31–36.

[6] S. Capell, S. Green, B. Curless, T. Duchamp, and Z. Popović, “A multiresolution framework for dynamic deformations,” in *Proc. SIGGRAPH/Eurographics Symposium on Computer Animation*, 2002, pp. 41–47.

[7] E. Grinspun, P. Krysl, and P. Schroder, “Charms: A simple framework for adaptive simulation,” in *Proc. Annual conference on Computer Graphics and Interactive Techniques (SIGGRAPH 02)*, 2002, pp. 281–290.

[8] M. Cavusoglu and F. Tendick, “Multirate simulation for high fidelity haptic interaction with deformable objects in virtual environments,” in *Proc. Robotics and Automation*, 2000, pp. 2458–2465.

[9] R.D. Cook, D.S. Malkus, and M.E. Plesha, *Concepts and Applications of Finite Element Analysis*, 3rd ed. John Wiley and Sons, 1989.

[10] O.C. Zienkiewicz, R.L. Taylor, and J.Z. Zhu, *The Finite Element Method: Its Basis and Fundamentals*, 6th ed. Elsevier Butterworth Heinemann, 2005.

[11] X.D. Pang, H.Z. Tan, and N.I. Durlach, “Manual discrimination of force using active finger motion,” *Perception and Psychophysics*, pp. 531–540, 1991.

[12] F. Barbagli, K. Salisbury, C. Ho, C. Spence, and H.Z. Tan, “Haptic discrimination of force direction and the influence of visual information,” *ACM Trans. Appl. Perception*, vol. 3, pp. 125–135, 2006.

[13] U. Koçak, K. Palmerius, and M. Cooper, “Dynamic deformation using adaptable, linked asynchronous fem regions,” in *Proc. Spring Conference on Computer Graphics*, 2009, pp. 213–220.

[14] G. Picinbono, H. Delingette, and N. Ayache, “Non-linear anisotropic elasticity for real-time surgery simulation,” *Graph. Models*, pp. 305–321, 2003.

[15] V. Egorov, S. Tsyuryupa, S. Kanilo, M. Kogit, and A. Sarvazyan, “Soft tissue elastometer,” *Medical Engineering and Physics*, pp. 206–212, 2008.

[16] X. Li, G. Wang, L. Huang, and G. Zhang, “Young’s modulus extraction methods for soft tissue from ultrasound measurement system,” *Instrumentation Science and Technology*, pp. 393–404, 2006.

[17] R. Sinkus, J. Lorenzen, D. Schrader, M. Lorenzen, M. Dargatz, and D. Holz, “High-resolution tensor mr elastography for breast tumour detection,” *Physics in Medicine and Biology*, pp. 1649–1664, 2000.

[18] A. Samani, J. Bishop, C. Luginbuhl, and D.B. Plewes, “Measuring the elastic modulus of ex vivo small tissue samples,” *Physics in Medicine and Biology*, pp. 2183–2198, 2003.

[19] P.C. Johns and M.J. Yaffe, “X-ray characterisation of normal and neoplastic breast tissues,” *Physics in Medicine Biology*, pp. 675–695, 1987.

[20] J.M. Wakeling and B.M. Nigg, “Soft-tissue vibrations in the quadriceps measured with skin mounted transducers,” *Journal of Biomechanics*, vol. 34, pp. 539–543, 2001.

[21] G. Rus and J.G. Martnez, “Ultrasonic tissue characterization for monitoring nanostructured tio2-induced bone growth,” *Physics in Medicine and Biology*, vol. 52, pp. 3531–3547, 2007.

[22] A. Field, *Discovering Statistics Using SPSS*, 2nd ed. Sage Publications Ltd, 2005.

[23] R.N. Stiles and J.E. Randall, “Mechanical factors in human tremor frequency,” *Applied Physiology*, vol. 23, pp. 324–330, 1967.

[24] M.A. Srinivasan and J.S. Chen, “Human performance in controlling normal forces of contact with rigid objects,” in *Winter Annual Meeting of the American Society of Mechanical Engineers*, 1993, pp. 119–125.

[25] T.L. Brooks, “Telerobotic response requirements,” in *IEEE Int. Conf. on Systems, Man, and Cybernetics*, 1990, pp. 113–120.

 ISBN: 978-1-61208-177-9 